Sub-degree CMB anisotropies from inflationary bubbles

Carlo Baccigalupi

INFN and Dipartimento di Fisica, Via del Paradiso 12, 44100, Università di Ferrara; Osservatorio Astronomico di Roma, Viale del Parco Mellini, 84, 00136 Roma

Received ______________________; accepted ______________________

ABSTRACT

It is well known that processes of first order phase transitions may have occurred in the inflationary era. If one or more occurred well before the end of inflation, the nucleated bubbles are stretched to large scales and the primordial power spectrum contains a scale dependent non-Gaussian component provided by the remnants of the bubbles. We predict the anisotropies in the cosmic microwave background (CMB) induced by inflationary bubbles. We build a general analytic model for describing a bubbly perturbation; we evolve each Fourier mode using the linear theory of perturbations from reheating until decoupling; we get the CMB anisotropies by considering the bubbly perturbation intersecting the last scattering surface. The CMB image of an inflationary bubble is a series of concentric isothermal rings of different color (sign of $\delta T/T$) on the scale of the sound horizon at decoupling ($\leq 1^o$ in the sky); the resulting anisotropy is therefore strongly non-Gaussian. The mean amplitude of $\delta T/T$ for a bubble of size L follows the known estimates for linear perturbations, $\delta T/T \simeq \delta\rho/\rho \cdot (L/H^{-1})^2$. In particular, bubbles with size corresponding to the seeds of the observed large scale voids (tens of comoving Mpc) induce an interesting pattern of CMB anisotropies on the sub-degree angular scale, to be further investigated and compared with the forthcoming high resolution CMB maps provided by the MAP and the Planck experiments.

Subject headings:

1. Introduction

Inflation is a phase of accelerated expansion driven by very high energy quantum fields ($kT \simeq 10^{15}$ GeV), which leaves observable cosmological traces at the present. The perturbations we observe today in the universe are therefore the most direct link we have to very high energy physics. Today, this fundamental topic is under investigation from several points of view: the perturbations imprinted on the cosmic microwave background (CMB) at the recombination era, the possible traces on the cosmic background of gravitational waves, the direct reconstruction of the three dimensional matter distribution traced by galaxies and their peculiar velocities in the modern redshift surveys and others.

The existence of large voids in the galaxy distribution, known for a long time (Vogeley et al. 1991, Kauffmann & Fairall, 1991), is now being established quite firmely. Recently, several almost spherical voids with mean diameter of $40h^{-1}$ Mpc have been detected and catalogued in the SSRS2 survey (El-Ad, Piran & da Costa, 1996); the surrounding walls have a thickness smaller than $10h^{-1}$ Mpc; the largest voids reach the spatial limits of the survey and their fraction of volume is about 40%; if smaller voids are also considered the voids volume fraction has a lower limit of 75%. These amazing results are confirmed by the analysis on IRAS (El-Ad, Piran & da Costa, 1997); these papers contain very impressive pictures reproducing the large voids in a three dimensional view. Although rare isolated faint galaxies are found inside the voids, preliminary analysis of the peculiar velocities of the walls galaxies (Da Costa et al. 1996) indicate the almost complete absence of matter (baryonic and dark) in the central cavities. The matter is therefore confined between the voids, and this surely affects the cluster distribution, that recently has been found more correlated than expected (see e.g. Einasto J. et al. 1997 and references therein); also, the matter distribution on $\sim 100h^{-1}$ Mpc is revealing an evidence of extra power (Landy et al. 1996). The observed inhomogeneities constrain the minimal inflationary scenario (slow rolling and purely Gaussian fluctuations, see Padmanabhan 1993) and the consequences upon the viable parameter space are currently under investigation (Retzlaff et al. 1997 and references therein). Topological defects provided mainly by *post*-inflationary phase transitions (Pen et al. 1997, Durrer et al. 1996 and references therein), have been proposed to be the seeds for the observed inhomogeneities, and their CMB imprints have been predicted (Turok et al. 1997, Durrer et al. 1996); however, recent results revealed some power deficit both on the CMB and on the perturbations spectrum (Albrecht et al. 1997). A distinctive feature of these models is a non-Gaussian perturbation spectrum; non-Gaussianity means that the phases of the components of the perturbations are correlated in some way. Getting ready to detect eventual non-Gaussianity in the CMB high resolution maps provided by the next experiments is a non-trivial theoretical challenge that is currently under development (Ferreira & Magueijo 1997, Amendola 1996 and references therein).

This paper aims at predicting the CMB anisotropies generated by models of first order inflation in which the perturbation spectrum is in general the sum of the Gaussian slow rolling fluctuations and the scale dependent non-Gaussian perturbations from the remnants of nucleated bubbles. First order phase transitions in the early universe are predicted by many inflationary theories (see Kolb 1991), and one of the most interesting ideas introduced in inflationary cosmology in recent years is that in general the phase transition occurs *during* the inflationary slow rolling (Occhionero & Amendola 1994,Amendola et al. 1996). Like in ordinary first order inflation, the nucleated bubbles grow as the causal horizon until the collision with other bubbles stops the overcomoving growth; however in these models the true vacuum energy is not zero, thus the bubbles may be in the linear regime and, most important, the amount of $e-$foldings between the phase transition and the end of inflation allows the bubbles to grow comovingly. This phenomenology has very interesting consequences for what concerns the gravitational radiation produced by the colliding bubbles: the characteristic peak frequency, exponentially redshifted by inflation, may fall in a detectable range (Baccigalupi et al. 1997). At reheating, the energy stored in the bubble wall is converted in matter and radiation, leaving a bubbly trace in the cosmic density. In the case in which a phase transition occurred at about 50 e-foldings before the end of inflation, the remnants of the bubbles have comoving sizes of tens of Mpc; they could be the seeds of the large voids observed today, a possibility firstly suggested in La 1991 and then further investigated (see e.g. Amendola et al. 1996, Occhionero et al. 1997).

In a previous work (Baccigalupi, Amendola & Occhionero 1997) we computed the CMB anisotropies induced by non-linear voids and we obtained from COBE data an upper limit of about $100h^{-1}$ Mpc to the present radius of a non-linear void sitting on the last scattering surface (LSS); in Occhionero et al. 1997 we considered mainly the time evolution of spherical bubbles in the matter dominated era, as the outcome of linear ones at decoupling and also we obtained (again from COBE) an upper limit of about $100h^{-1}$ Mpc to the present radius of linear bubbles on the LSS. Here we compute the detailed CMB anisotropies generated by an inflationary bubble. We build an analytic model for describing a general linear bubbly perturbation;

we evolve each Fourier mode from reheating to decoupling using the theory of linear perturbations (see Hu & Sugiyama 1995 and references therein). Finally we get the CMB anisotropies by considering the intersection between the bubble and the LSS. We shall focus the analysis on bubble comoving sizes of tens of Mpc at decoupling (angular scale below 1^o), since they correspond to the observed structures and voids recently catalogued (El-Ad, Piran & da Costa, 1996,1997).

In Amendola et al. 1997 we consider a realistic CMB fluctuation field produced by a primordial power spectrum containing ordinary Gaussian fluctuations and a non-Gaussian bubbly component, as predicted by the first order inflation models mentioned above; the volume fraction ($\simeq 50\%$ at the present) occupied by the bubbles allow them to significatively affect the large scale structure: the impact of this model on the CMB angular power spectrum is predicted.

Our computations shall be compared with the high resolution CMB maps provided by the next MAP and Planck experiments, that will provide the whole sky CMB anisotropy maps down to $\delta T/T \simeq 10^{-6}$ and with angular resolution of $10^{'}$.

The paper is organized as follows: section II is dedicated to the analytical construction of the perturbation field; in Section III we apply the linear perturbation theory and evolve the bubbly perturbation from reheating until decoupling focusing on the corresponding perturbation in the photon baryon plasma; in Section IV we compute the bubbly CMB anisotropies; finally, Section V contains the conclusions.

2. A general analytic model

In principle, it is possible to calculate the exact bubble shape by considering a specific first order inflationary model and the fields involved in the process. However, since a bubbly density perturbation is specified by few parameters, we choose here to parametrize the inflationary bubble directely at reheating. Bubbles from a phase transition occurred early during inflation are stretched comovingly to large scales by the remaining inflation (Occhionero & Amendola 1994,Amendola et al. 1996). At reheating they leave a perturbation in the cosmic density. A compensated spherical bubble is described by its central density contrast δ, comoving radius R and thickness σ of the compensating shell:

$$\delta = \left|\frac{\delta\rho}{\rho}\right|_{r=0} \quad , \quad R \quad , \quad \sigma = \frac{\Delta R_{shell}}{R} \quad . \tag{1}$$

Defining a radial coordinate $x = r/R$ in the comoving gauge, we model naturally two zones in a bubble, the central underdensity and the compensating shell; the width of the latter is divided in inner (σ_i) and outer (σ_o), with $\sigma_i + \sigma_o = \sigma$. We model the bubble as follows:

$$\begin{aligned}
\frac{\delta\rho}{\rho} &= -\delta \quad (x \leq 1-\sigma_i) \quad , \\
\frac{\delta\rho}{\rho} &= A + B\sin\left[\frac{\pi}{\sigma_i}\left(x + \frac{\sigma_i}{2} - 1\right)\right] \quad (1-\sigma_i \leq x \leq 1) \quad , \\
\frac{\delta\rho}{\rho} &= C + D\sin\left[\frac{\pi}{\sigma_o}\left(x + \frac{\sigma_o}{2} - 1\right)\right] \quad (1 \leq x \leq 1+\sigma_o) \quad .
\end{aligned} \tag{2}$$

The constants are determined by the requests of continuity and compensation:

$$\begin{aligned}
D &= C = B - \frac{\delta}{2} = A + \frac{\delta}{2} = \\
&= \delta \quad \frac{\frac{1}{3}(1-\sigma_i)^3 + \frac{1}{6}\left[1-(1-\sigma_i)^3\right] - \frac{\sigma_i^2}{\pi^2}(2-\sigma_i)}{\frac{1}{3}\left[1-(1-\sigma_i)^3\right] + \frac{2\sigma_i^2}{\pi^2}(2-\sigma_i) + \frac{1}{3}\left[(1+\sigma_o)^3 - 1\right] - \frac{2\sigma_o^2}{\pi^2}(2+\sigma_o)} \quad .
\end{aligned} \tag{3}$$

The Fourier transform of the above density contrast in a volume V is

$$\left(\frac{\delta\rho}{\rho}\right)_k = \int \frac{\delta\rho}{\rho}(r)\frac{\sin kr}{kr}\frac{4\pi r^2 dr}{V} = -\frac{4\pi\delta}{Vk^3}\left[-y\cos y + \sin y\right]_0^{kR(1-\sigma_i)} \quad +$$

$$
\frac{4\pi A}{Vk^3}\left[-y\cos y+\sin y\right]_{kR(1-\sigma_i)}^{kR}+\frac{4\pi C}{Vk^3}\left[-y\cos y+\sin y\right]_{kR}^{kR(1+\sigma_o)}\quad -
$$
$$
\frac{2\pi B}{Vk(k+\pi/\sigma_i R)^2}\left[\left(y+\frac{\pi}{\sigma_i}-\frac{\pi}{2}\right)\sin y+\frac{\cos y}{k+\pi/\sigma_i R}\right]_{R(1-\sigma_i)(k+\pi/\sigma_i R)-\frac{\pi}{\sigma_i}+\frac{\pi}{2}}^{R(k+\pi/\sigma_i R)-\frac{\pi}{\sigma_i}+\frac{\pi}{2}}\quad -
$$
$$
\frac{2\pi B}{Vk(-k+\pi/\sigma_i R)^2}\left[\left(y+\frac{\pi}{\sigma_i}-\frac{\pi}{2}\right)\sin y+\frac{\cos y}{-k+\pi/\sigma_i R}\right]_{R(1-\sigma_i)(-k+\pi/\sigma_i R)-\frac{\pi}{\sigma_i}+\frac{\pi}{2}}^{R(-k+\pi/\sigma_i R)-\frac{\pi}{\sigma_i}+\frac{\pi}{2}}\quad -
$$
$$
\frac{2\pi D}{Vk(k+\pi/\sigma_o R)^2}\left[\left(y+\frac{\pi}{\sigma_o}-\frac{\pi}{2}\right)\sin y+\frac{\cos y}{k+\pi/\sigma_o R}\right]_{R(k+\pi/\sigma_i R)-\frac{\pi}{\sigma_o}+\frac{\pi}{2}}^{R(1+\sigma_o)(k+\pi/\sigma_o R)-\frac{\pi}{\sigma_o}+\frac{\pi}{2}}\quad -
$$
$$
\frac{2\pi D}{Vk(-k+\pi/\sigma_o R)^2}\left[\left(y+\frac{\pi}{\sigma_o}-\frac{\pi}{2}\right)\sin y+\frac{\cos y}{-k+\pi/\sigma_o R}\right]_{R(-k+\pi/\sigma_o R)-\frac{\pi}{\sigma_o}+\frac{\pi}{2}}^{R(1+\sigma_o)(-k+\pi/\sigma_i R)-\frac{\pi}{\sigma_o}+\frac{\pi}{2}}\quad . \tag{4}
$$

This model allows for the description of any compensated spherical underdensity with the choice of parameters δ, R and σ_i, σ_o. Figure (1) shows the radial density contrast (top) and the corresponding Fourier transform (bottom) for different shapes. Note that the latter is strongly scale dependent: it is characterized by a peak at $k \simeq 2\pi/2R$, corresponding to the diameter of the bubble. On smaller wave numbers, the spectrum falls as k, while the oscillations at higher k describe the compensating shell. Left panels display the dependence on the shell width by maintaining $\sigma_i = \sigma_o$; right panels display the analysis of asymmetric shells $\sigma_i \neq \sigma_o$. The variation of width and shape of the compensating shell does not affect substantially the amplitude and the oscillating behaviour of the Fourier transform. This makes the results of the next Sections almost independent of the exact shell shape; for this reason we put the emphasis on the more interesting physical observables R and δ, and simply assume $\sigma = 2\sigma_i = 2\sigma_o = .3$ (the solid lines in Fig.(1)). Also, independent reasons to neglect the dependence on the shell's shape arise from CMB damping of anisotropies on very small angular scales (Silk damping), to be described in the next Section. Finally, note that the perturbation (and its CMB counterpart) scales linearly with δ, that has been factored out in the axis labels.

In the next Section we shall consider the perturbation described here in the cosmic medium at reheating and we will evolve it until decoupling.

3. From reheating to decoupling

Here we want to compute in detail the CMB perturbations induced by the remnants of inflationary bubbles from reheating until decoupling, leaving to the next Section the analysis of the corresponding CMB anisotropies. We perform the computations in a standard scenario (flat CDM, low baryon density ($\Omega_b = .06$), h=.5). As in Baccigalupi, Amendola & Occhionero 1997 we adopt the approach developed in Hu & Sugiyama 1995, since it is applicable to any kind of scalar linear perturbation and very accurate ($5 \div 10\%$). We report here only the basic and intuitive features of the method.

Let us consider the Fourier modes (4) as initial condition in the matter distribution at reheating. Let the scale factor be $a(\eta)$ and the time variable be the conformal time $\eta = \int_0^t d\tau/a(\tau)$,. Each mode $(\delta\rho/\rho)(k,\eta)$ evolves according to the linear theory of perturbation and its gravitational potential induces the corresponding time evolving perturbation $(\delta T/T)(k,\eta)$ in the photon baryon plasma. At decoupling, the latter imprints anisotropies $(\delta T/T)(\theta,\phi)$ in the CMB. Summarizing, the process involves the following steps:

$$
\frac{\delta\rho}{\rho}(k,0)\rightarrow\frac{\delta T}{T}(k,0)\rightarrow \text{evolution}\rightarrow\frac{\delta T}{T}(k,\eta_D)\rightarrow\frac{\delta T}{T}(\theta,\phi)\quad . \tag{5}
$$

The photon-baryon plasma contains zero-point adiabatic $(\delta T/T)_0(k,\eta)$ and pure velocity $V(k,\eta)$ perturbations; at decoupling the Sachs-Wolfe effect (SW, $(\delta T/T)_{SW}(k,\eta)$) given simply by the gravitational potential, must be added. In the tight coupling approximation, the equations driving the time evolution are

(Hu & Sugiyama 1995)

$$\left(\frac{\delta \ddot{T}}{T}\right)_0 + \frac{\dot{a}}{a}\frac{\mathcal{R}}{1+\mathcal{R}}\left(\frac{\delta \dot{T}}{T}\right)_0 + \frac{k^2}{3(1+\mathcal{R})}\left(\frac{\delta T}{T}\right)_0 = -\ddot{\Phi} - \frac{\dot{\mathcal{R}}}{1+\mathcal{R}}\dot{\Phi} - \frac{k^2}{3}\Psi \quad , \tag{6}$$

$$V = -\frac{3}{k}\left[\left(\frac{\delta \dot{T}}{T}\right)_0 + \dot{\Phi}\right] \quad , \quad \left(\frac{\delta T}{T}\right)_0 (\eta = 0) = -\frac{\Psi(0)}{2} \ , \ V(0) = 0 \quad , \tag{7}$$

where dot denote derivative with respect to η. The quantity $\mathcal{R}$ is $3\rho_b/4\rho_\gamma$ (the subscripts b, γ refer to baryons and photons respectively), and $r_s(\eta) = \int_0^\eta d\eta'/\sqrt{3(1+\mathcal{R})}$ is the sound horizon at η. The gravitational potentials are

$$\Phi = (1+z)\frac{3H_0^2}{2k^2}\left(\frac{\delta\rho}{\rho}\right)(k,\eta) \simeq -\Psi \quad ; \tag{8}$$

the little difference between Φ and Ψ, due to the radiation components of the cosmic fluids, is taken into account in the computations. Below the Silk damping scale, the photon baryon plasma perturbations are damped by a factor $\exp[-k^2/k_D^2(\eta)]$, where the damping scale k_D^{-1} is of the order of ten comoving Mpc at decoupling and soon there after grows to the horizon scale. We simply put the spectrum (4) as the initial density perturbation; through linear theory, encoded for the CMB in (67), we follow its evolution until decoupling.

The above procedure allows to perform the first three steps indicated in (5); however, since the perturbations here are non-Gaussian, the computation of the CMB angular anisotropies can not be done automatically as for Gaussian perturbations, but requires some more details, that we leave to the next Section. Note that the above procedure is general and does not depend on the particular initial perturbation spectrum; therefore the CMB perturbation resulting from the evolution of any non-Gaussian linear feature from reheating may be calculated from its Fourier transform using the above procedure. Also, because of linearity, the time evolution of our bubbles or any kind of non-Gaussian perturbations present in the cosmic fluid at reheating does not depend on the presence of another (e.g. Gaussian) component in the perturbation spectrum. This is of particular interest for first order inflation models which provide two independent perturbation mechanisms, (bubbles and Gaussian fluctuations from the slow rolling field in the present case) as already mentioned in the Introduction.

Let us concentrate now on the CMB perturbations induced by bubbles. We evolve the photon baryon perturbations until decoupling, when we antitransform to get the relevants effects as a function of r. Figure (2) shows the adiabatic (top), Doppler (middle) and SW effect (bottom). The bubbles under investigation are charecterized by a central density contrast δ at decoupling that we put on the y-axis units, and by $R = 10, 15, 20h^{-1}$ Mpc; these radii are comparable with the size of the observed large voids in the galaxy distribution (El-Ad, Piran & da Costa, 1996,1997). The most interesting feature of the results shown in Fig.(2) can be noted by looking at the curves and the scales: the SW effect strictly does not extend beyond the size of the perturbation, while the adiabatic and Doppler ones are not vanishing until $60 \div 80h^{-1}$ Mpc from the center of the bubble, *independently* of its radius. This is infact the amplitude of the sound horizon of the photon-baryon plasma at decoupling. Just like a pebble in a pond, the initial small bubbly perturbation is propagating beyond the initial scale, reaching the scale of the sound horizon at the time in which we are examinating it. A sound wave with negative and positive crests is well evident at the sound horizon position, both in the adiabatic and Doppler effects. We have further investigated the motion of this wave for the case $R = 20h^{-1}$ Mpc. Fig.(3) shows in detail the wave at different times. Two physically expected effects are immediately evident: the wave is travelling outward the bubble and simultaneously damped due to the Silk damping, that is becaming more and more active with time.

Also note as the SW effect (and roughly the adiabatic one) follows the known amplitude (Padmanabhan 1993) for linear perturbations $\delta T/T \simeq -\delta(R/H^{-1})^2$. We have not found a significative dependence on the shell's shape: for instance, by taking $\sigma' = \sigma/2$ and repeating the same computations, the results change of a few percent; this is due to the Silk damping, the effect of which is to erase the small scale CMB anisotropies at decoupling; in fact, the damping exponential mentioned above is $1/e$ at about $10h^{-1}$ Mpc in the present CDM model; thus, the damping is particularly effective on the small scales involved by the shell (a few comoving Mpc).

As we will see in the next Section, the above results imply that the CMB anisotropies of an inflationary linear bubble consist in general in a few concentric rings of alternate colour (sign of $\delta T/T$) on the sub-degree angular scale.

4. Anisotropies

The perturbations in the photon-baryon plasma are photographed at last scattering and described by the CMB anisotropy field:

$$\frac{\delta T}{T}(\theta,\phi)=\sum_{lm}a_{lm}Y_{lm}(\theta,\phi)\quad . \tag{9}$$

Concerning the anisotropy amplitude, the physical information is contained in the correlation function

$$C(\theta)=\left\langle\left(\frac{\delta T}{T}\right)_{\mathbf{n}}\left(\frac{\delta T}{T}\right)_{\mathbf{n}'}\right\rangle_{\mathbf{nn}'=\cos\theta}=\sum_{l}\frac{\sum_m|a_{lm}|^2}{4\pi}P_l(\cos\theta)\quad , \tag{10}$$

where P_l are the Legendre polynomials and the average is taken over all the sky directions $\mathbf{n}$ and $\mathbf{n}'$ separated by the angle θ. The coefficients $\sum_m|a_{lm}|^2$ are conventionally renamed as $(2l+1)C_l$ in a Gaussian theory; for the functional properties of the P_l, the $l-$th coefficient describes the CMB anisotropies at the angular scale $\theta=\pi/l$ (see White et al., 1994 and references therein). The coefficients C_l of the expansion in Legendre polynomials do not determine uniquely the anisotropies, but only their amplitude at a given angular scale specified by l; they completely neglect the phases of the a_{lm} coefficients, and therefore describe the anisotropies only if the phases are randomly distributed (Gaussian perturbations). If on the contrary the anisotropies are the outcome of some coherent, i.e. non-Gaussian, structure, the C_l are indicative of the amplitude only, but not of the coherence. This point is of particular interest in Amendola et al. 1997, where the subject is the impact of a bubbly distribution on the C_l spectrum.

Here we want to compute the CMB anisotropies (9) generated by remnants of inflationary bubbles. On a particular direction $\mathbf{n}$, the anisotropy is given by

$$\left(\frac{\delta T}{T}\right)_{\mathbf{n}}=\int_0^{\eta_o}\left(\frac{\delta T}{T}\right)_{\mathbf{n}}(\eta)P(\eta)d\eta\quad , \tag{11}$$

where $P(\eta)$ is the probability for a photon to be last scattered between times η and $\eta+d\eta$; $(\delta T/T)_{\mathbf{n}}(\eta)$ is the CMB perturbation field at causal distance $\eta_0-\eta$ on the direction $\mathbf{n}$. The perturbations examined here are spatially localized: they have a center and vanish beyond a sound horizon distance from it. Consequentely, in performing the computation (11), we must specify the position of the bubble's center with respect to the LSS. We choose to orient the polar axis towards the center of the bubble, so that due to its spherical symmetry, the anisotropy field (9) is a function only of the polar angle θ, that is the angle between the bubble center direction and the particular line of sight $\mathbf{n}$; the same angular choice was made in Baccigalupi, Amendola & Occhionero 1997. The remaining degree of freedom regards the distance of the bubble on the line of sight; its perturbation on the CMB depends on the distance of the bubble's center from the LSS (hereafter d) and vanishes of course if the perturbing zone does not intersects the LSS: to exemplify this dependence, we shall display in the sequel three interesting cases: $d=-R,0$ and $+R$. Let us consider a photon last scattered at some η inside the bubble and running towards the observation point on some direction θ; the $\delta T/T$ that it carries depends on several variables: θ, d and η uniquely determine the radial coordinate (radial with respect to the bubble's center of course) at which it decouples; we compute the adiabatic, SW and Doppler effects and the overall CMB perturbation

$$\frac{\delta T}{T}(\theta,d,\eta)=\left(\frac{\delta T}{T}\right)_0+\left(\frac{\delta T}{T}\right)_{SW}+V\cdot\cos\alpha\quad , \tag{12}$$

where α is the angle between the radial direction and the line of sight, and of course accounts for the direction dependence of the Doppler effect. The above expression means that for each η we antitransform $(\delta T/T)(k,\eta)$ as obtained from the procedure of the previous Section. Note that this is particularly accurate, since the behaviour of the Silk damping scale (that suddenly after the decoupling grows up to the horizon

scale) is taken into account. Finally we get the CMB anisotropies simply averaging on all η's, weighted with the last scattering probability $P(\eta)$ (11). The integrated SW effect, due to the time change of the gravitational potential while the photon crosses the bubble, is not taken into account since it is completely negligible, as in the non-linear case (Baccigalupi, Amendola & Occhionero 1997).

Figure (4) reports the CMB anisotropies from bubbles lying on the LSS; the radii are the same as in Fig.(2). In each panel, three different lines show the interesting variation of the angular dependence of $\delta T/T$ with the relative positions of the LSS with respect to the bubble's center: $d = -R, 0, +R$ (respectively short dashed, solid and long dashed). Of course the whole signal scales with δ and grossly the features of Fig.(2) are respected. Note the effects of the variation of d: the negative strong spot near the center, coming mainly from the adiabatic effect (see also Fig.(2)), is depressed if the bubble is displaced behind or beyond the LSS.

Finally in Figure (5) the CMB sky contains only one bubble with $R = 20h^{-1}$ Mpc and $\delta = .005$ (top), $\delta = .01$ (bottom), lying on the LSS, corresponding to the solid line on the bottom panel in Fig.(4); in the same sky region we have added a purely Gaussian $\delta T/T$ from the standard CDM model. The spherical imprint provided by the bubble is well evident in the bottom panel, but rather hidden in the top panel, depending of course on δ. Note however that both bubbles become strongly non-linear at the present, and therefore are able to affect substantially the structure formation (Occhionero et al. 1997). The signal shows clearly its marked non-Gaussianity: the sound wave propagating outward and the central spot generated by SW and adiabatic effect determine the appearance of a few fascinating concentric rings of alternate colour on the sub-degree angular scale. As the mean anisotropy amplitude in Fig.(5) is not different from the ordinary Gaussian case, the distinctive imprints of these structures on the CMB are to sought not as much in the anisotropy amplitude (10), but rather in the phase correlation encoded in higher order statistics.

The above results have to be extended to a realistic distribution of bubbles. The resulting maps will be compared with the present and next high resolution CMB observations. We leave these analysis to forthcoming works, beginning with the impact on the C_l (10), in Amendola et al. 1997.

5. Conclusions

The occurrence of first order phase transitions in the early universe is largely predicted, and its indirect detection through the present observable traces would be of crucial importance for our understanding of fundamental physics. If one or more of such processes occurs well before the end of inflation, the nucleated bubbles are stretched to large scales; this has very important consequences on the observability of these very high energy physics phenomena. Here we predict the traces left by inflationary bubbles on the CMB. To achieve this aim, we first model analytically a bubble. We use the general linear theory to get the Fourier transform of the corresponding perturbation in the photon baryon plasma and to evolve it until decoupling. Then, by considering a CMB photon decoupled at some point inside the bubble, we antitransform to get the $\delta T/T$ carried by the photon; by repeating the above computation for each direction and for each decoupling point weighted with the last scattering probability function, we get the whole CMB anisotropy produced by an inflationary bubble.

We find that the CMB perturbation propagates on the scale of the sound horizon at decoupling ($\simeq 1^o$ in the sky), and appears as a fascinating series of concentric rings of alternate color (different sign of $\delta T/T$), a general feature that remains true as the bubble is moved back and forth with respect to the last scattering surface. Therefore, in comparison with ordinary anisotropies from scale invariant perturbation spectra, the present signal presents a marked non-Gaussianity. The overall mean amplitude of the signal from a bubble with radius R and central density contrast $\delta \ll 1$ is of the order of $\delta(R/H^{-1})^2$, as expected for linear perturbations. Therefore, bubbles with comoving radii corresponding to the size of the observed large scale structures (tens of Mpc), and characterized by a central density contrast $\delta \simeq 10^{-3}$, induce a level of anisotropy to be interestingly compared with the observed ones.

If bubbles are produced during the inflationary era, the resulting fluctuation spectrum is a superposition of the standard Gaussian fluctuations from the slow rolling inflaton and the scale dependent non-Gaussian ones from the bubbles. The results of the present paper will be used to make quantitative predictions of the imprint of these inflationary models on the CMB. Since the angular scale involved by the bubbles are well below 1^o, our computations shall be compared with the high resolution CMB maps provided by the next MAP and Planck experiments.

I wish to thank Luca Amendola, Pierluigi Fortini and Franco Occhionero for their collaboration and warm encouragement.

REFERENCES

Albrecht A. et al. 1997 preprint, astro-ph/9707129

Amendola L., Baccigalupi C., Konoplick R., Occhionero F. & Rubin S. 1996 Phys. Rev. D 54 7199

Amendola L., Baccigalupi C. & Occhionero F. 1997 Ap.J.Lett. in press

Amendola L. & Borgani S. 1994 MNRAS 266, 191

Amendola L. & Occhionero F. 1993 Ap.J. 413, 39

Baccigalupi C., Amendola L. Fortini P. & Occhionero F. 1997 Phys.Rev.D 56 4610, gr-qc/9709044

Baccigalupi C., Amendola L. & Occhionero F. 1997 MNRAS 288 387

Da Costa L.N., Freudling W., Wegner G., Giovanelli R., Haynes M., and Salzer J.J. 1996 Ap.J. 468, L5

Einasto J. et al. 1997 Nature 385 139

El-Ad H., Piran T. & da Costa L. N., 1996 Ap.J. 462, L13

El-Ad H., Piran T. & da Costa L. N., 1997 MNRAS 287 790

Ferreira P.G. & Magueijo J. 1997 Phys.Rev.D 55, 3358; Amendola L. 1996 MNRAS 283, 983

Kolb E.W. 1991 Physica Scripta T36, 199

Hu W. & Sugiyama N. 1995 Ap.J. 444, 489

La D. 1991 Phys.Lett. B 265, 232

Landy S. D., Shectman S. A., Lin H., Kirshner R. P., Oemler A. A. & Tucker D. 1996 Ap.J. 456, L1

Occhionero F. & Amendola L. 1994 Phys.Rev. D 50 4846

Occhionero F, Baccigalupi C., Amendola L., Monastra S. 1997 Phys.Rev.D, in press

Padmanabhan T.,Structure formation in the universe, Cambridge university press 1993

Pen U., Seljak U. & Turok N. Phys.Rev.Lett. 79, 1611; Durrer R. & Zhou Z., H., 1996 Phys.Rev. D 53, 5394

Retzlaff J., Borgani S., Gottloeber S. & Mueller V. 1997 astro-ph/9709044 submitted to MNRAS

Turok N., Pen U. & Seljak U. 1997 astro-ph/9706250; Durrer R. et al. 1996 Phys.Rev.Lett. 75, 579

Vogeley M. S., Geller M. J. & Hucra J. P. 1991 Ap.J. 382, 54; Kauffmann G. & Fairall A. P. 1991 MNRAS 248, 313

White M., Scott D. & Silk J. Annu. Rev. Astron. and Astrophys. 1994 32, 319

Fig. 1.— Radial density profiles (top panels) and their Fourier transforms (bottom panels). The overall properties of the k-spectrum are almost the same in any of the case shown. Examples of symmetric shells

---

This manuscript was prepared with the AAS LaTeX macros v4.0.

($\sigma_i = \sigma_o = \sigma/2$) are on the left: $\sigma = .2$ (short dashed line), $\sigma = .3$ (solid line) and $\sigma = .5$ (long dashed line) Cases of asymmetric shells are on the right: $\sigma_i = .2$, $\sigma_o = .1$ (short dashed line), $\sigma_i = \sigma_o = .15$ (solid line) and $\sigma_i = .1$, $\sigma_o = .2$ (long dashed line).

Fig. 2.— CMB perturbations at decoupling induced by an inflationary bubble: adiabatic effect in the top, Doppler in the middle, and Sachs-Wolfe in the bottom panel. The different lines refer to different radii as indicated. The Sachs-Wolfe effect does not exceed the bubble size, while the other effects generally extend on the sound horizon for the photon baryon plasma at decoupling.

Fig. 3.— The outward traveling waves in the adiabatic (top) and Doppler (bottom) effects for a bubble with $R = 20h^{-1}$ Mpc at different redshifts. The reduction of the amplitude is due to the Silk damping, that is becaming more and more active with time.

Fig. 4.— CMB anisotropies induced by bubbles of interesting size near the LSS in different positions: $d = -R$ (short dashed line), $d = 0$ (solid line) and $d = +R$ (long dashed line). The signal scales linearly with the central density contrast and involves angular scales up to 1^o.

Fig. 5.— A portion of microwave sky containing a purely Gaussian CDM $\delta T/T$ field together with the signature of an inflationary bubble with $R = 20h^{-1}$ Mpc, $\delta = .005,\ .01$ (respectively top and bottom) and sitting exactly on the LSS ($d = 0$). Horizontal scale is in acminutes. Although the spherical imprint is well evident in the bottom panel but only hidden in the top one, both bubbles are non-linear by the present and capable to affect substantially the large scale structure.

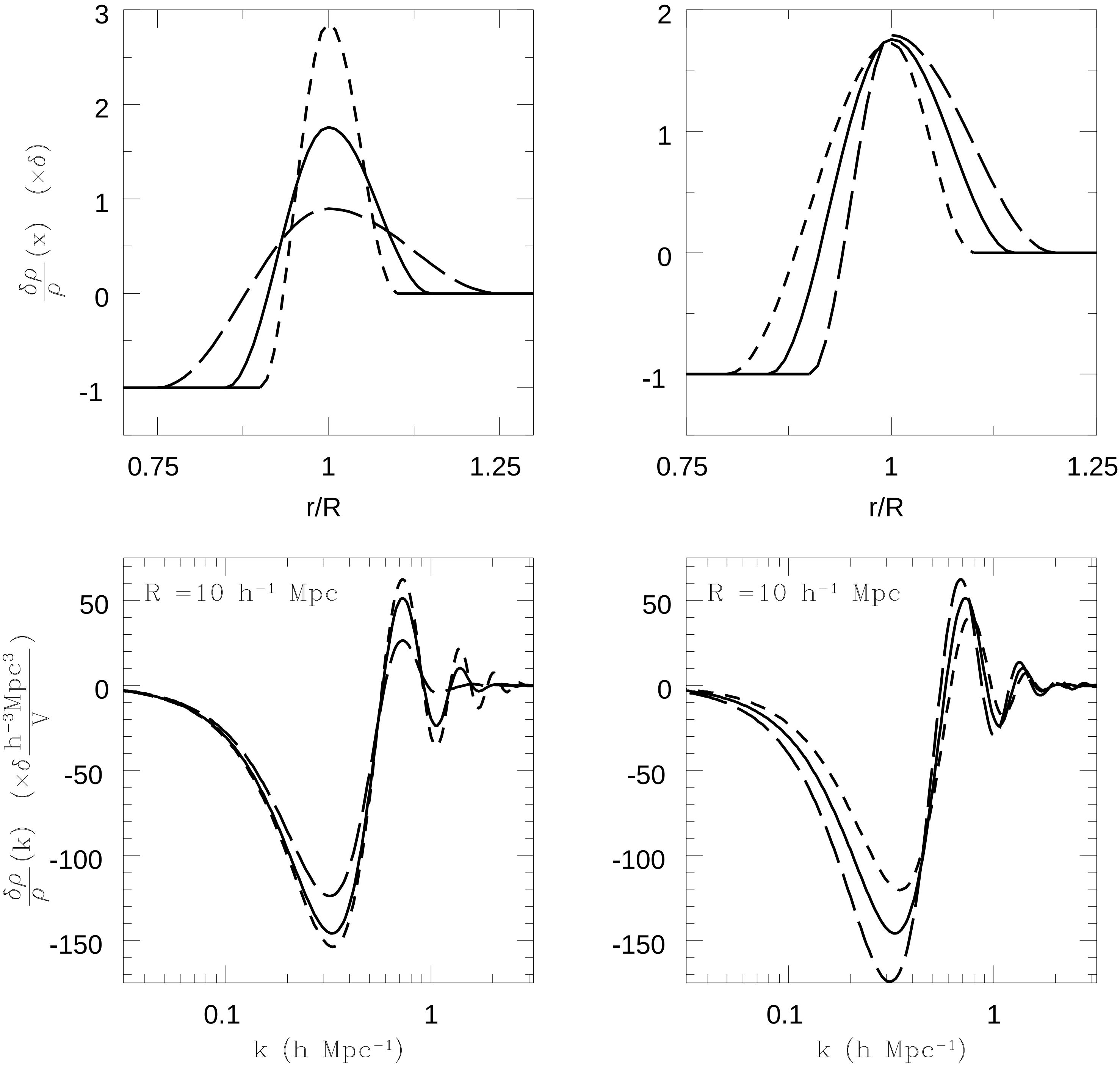

3
2
1
0
-1
$\frac{\delta\rho}{\rho}(x)$ $(\times\delta)$
0.75
1
1.25
r/R
2
1
0
-1
0.75
1
1.25
r/R
R =10 h⁻¹ Mpc
50
0
-50
-100
-150
$\frac{\delta\rho}{\rho}(k)$ $(\times\delta\frac{h^{-3}Mpc^3}{V})$
0.1
1
k (h Mpc⁻¹)
R =10 h⁻¹ Mpc
50
0
-50
-100
-150
0.1
1
k (h Mpc⁻¹)

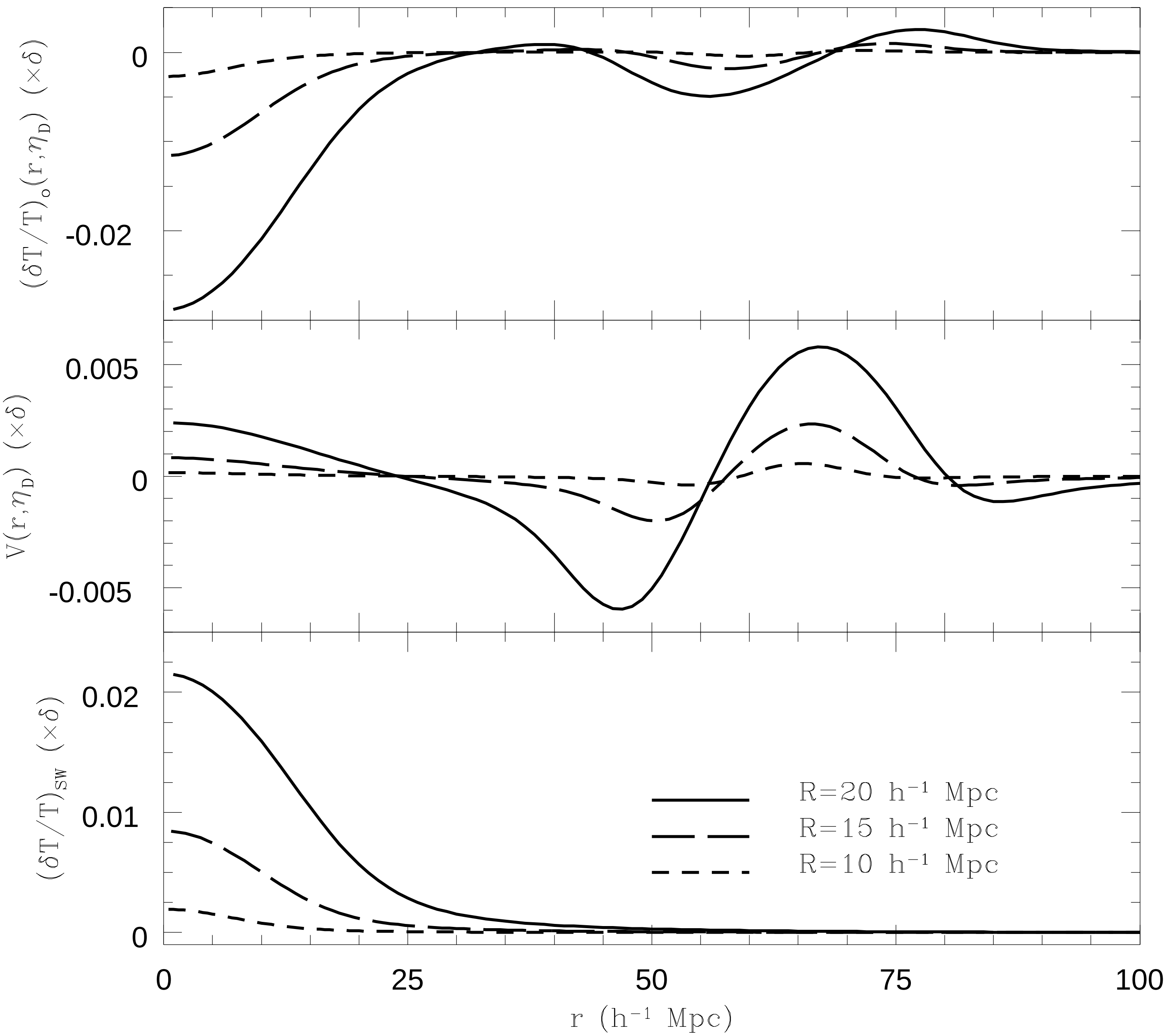

0
-0.02
$(\delta T/T)_o(r,\eta_D)$ $(\times\delta)$
0.005
0
-0.005
$V(r,\eta_D)$ $(\times\delta)$
0.02
0.01
0
$(\delta T/T)_{SW}$ $(\times\delta)$
R=20 h^{-1} Mpc
R=15 h^{-1} Mpc
R=10 h^{-1} Mpc
0
25
50
75
100
r (h^{-1} Mpc)

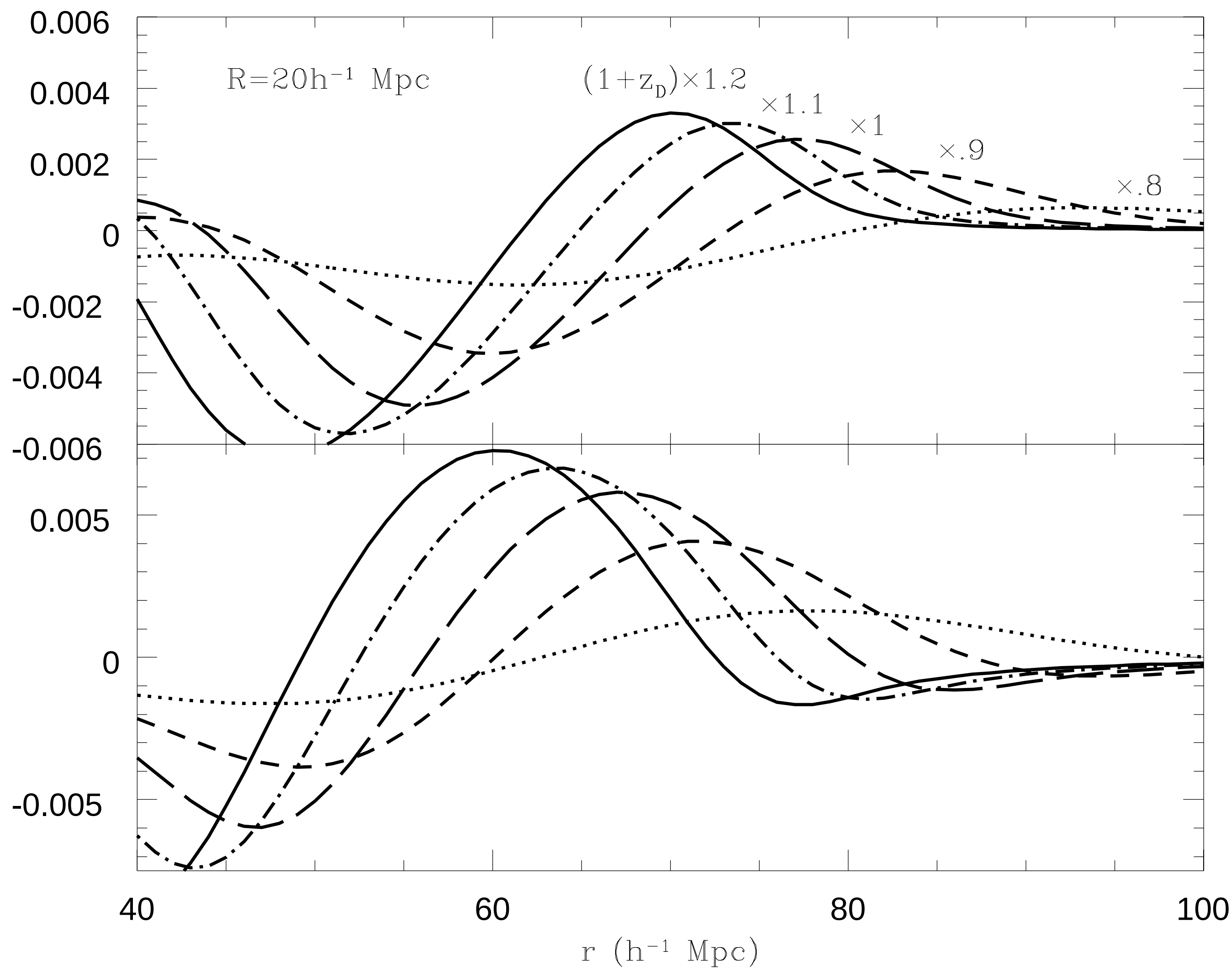

R=20h⁻¹ Mpc
(1+z_D)×1.2
×1.1
×1
×.9
×.8
(δT/T)_0(r,η) (×δ)
V(r,η) (×δ)
r (h⁻¹ Mpc)
0.006
0.004
0.002
0
-0.002
-0.004
-0.006
0.005
0
-0.005
40
60
80
100

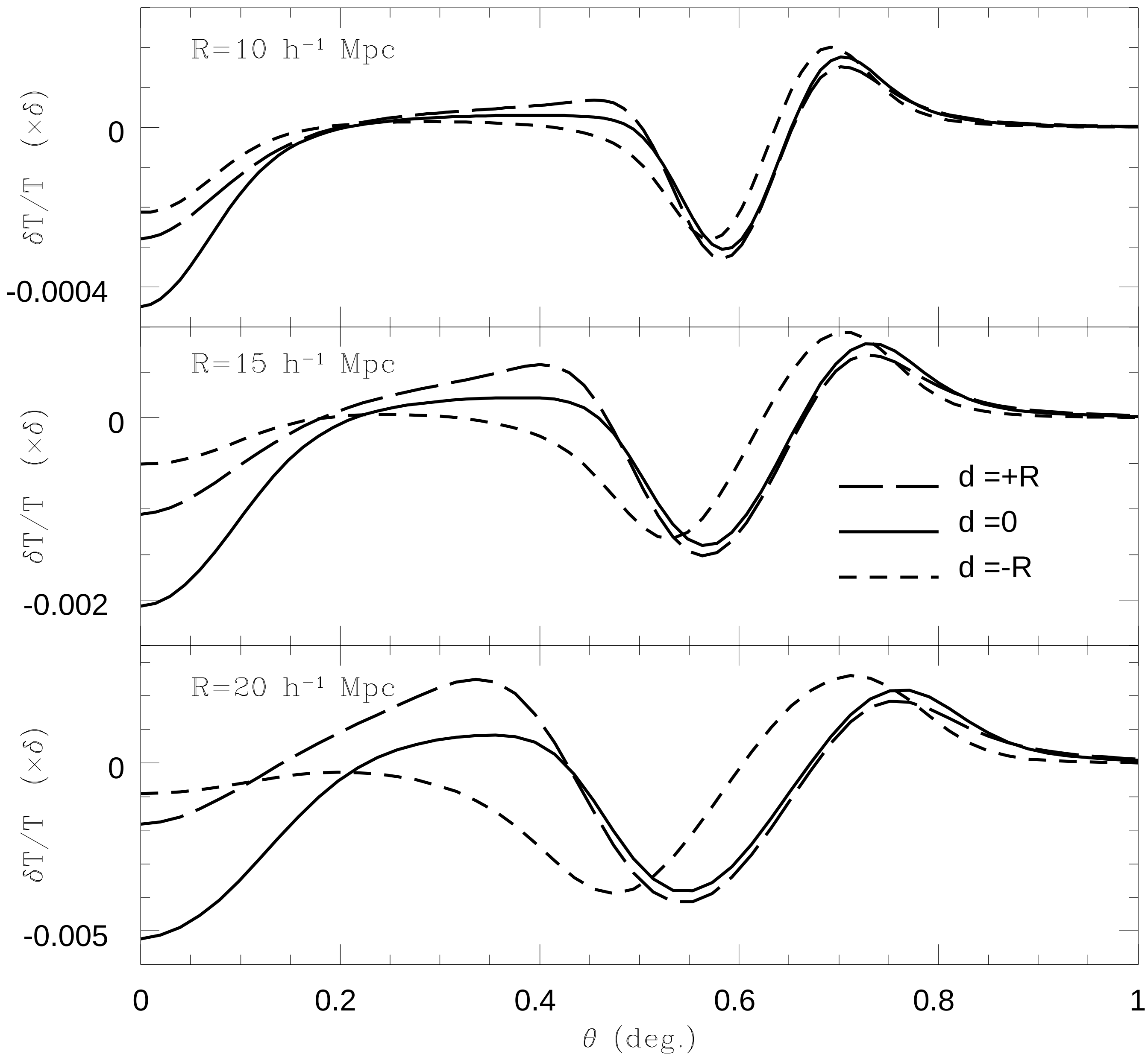

R=10 h⁻¹ Mpc
R=15 h⁻¹ Mpc
R=20 h⁻¹ Mpc
δT/T (×δ)
0
-0.0004
-0.002
-0.005
d =+R
d =0
d =-R
0
0.2
0.4
0.6
0.8
1
θ (deg.)

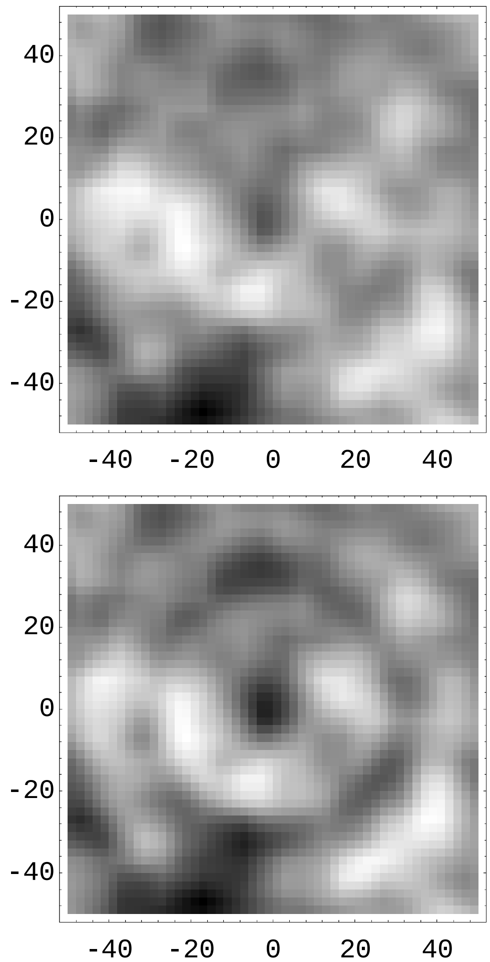
40
20
0
-20
-40
-40 -20 0 20 40
40
20
0
-20
-40
-40 -20 0 20 40